Article

New Self-Repairing System for Brittle Matrix Composites Using Corrosion-Induced Intelligent Fiber

Yuyan Sun [1], Dongkai Wang [1], Zuquan Jin [2], Jianwei Sun [1] and Ziguo Wang [1,*]

1   School of Civil Engineering, Qingdao University of Technology, Qingdao 266520, China
2   Engineering Research Center of Concrete Technology in Marine Environment, Ministry of Education, Qingdao University of Technology, Qingdao 266520, China
*   Correspondence: wangziguo@qut.edu.cn or wangziguo2008@163.com

Abstract: Brittle matrix composites such as concrete are susceptible to damage in the form of cracks. Most of the current self-repair and self-healing techniques have repair limits on crack widths or high costs of an external stimulator, or have an unfavorable effect on the composite's strength. This paper proposes a new concept of corrosion-induced intelligent fiber (CIF) and a new self-repairing system that uses the CIFs to close cracks in brittle matrix composites within a corrosive environment without external help, and without compromising the strength. The CIF comprises an inner core fiber and an outer corrodible coating that are in equilibrium, with the core fiber in tension and the corrodible coating in compression. The preparation steps and shape recovery mechanism of the CIF and the self-repair mechanism of the CIF composites are explained. Based on these concepts, this paper also describes several mechanical models built to predict the magnitude of pre-stress stored in the core fiber, and the maximum pre-stress released to the matrix composites, and the minimum length of the reliable anchor ends of CIF. The sample calculation results show that the recovery strain was 0.5% for the CIF with the steel core fiber and 12.7% for the CIF with the nylon core fiber; the maximum crack closing force provided by the CIF to concrete can be increased by increasing the amount of the CIFs in concrete and the initial tensile stress of the core fiber. This paper provides some suggestions for enhancing the self-repair capability of brittle composites in complex working environments.

Keywords: brittle matrix composites; concrete; corrosion; crack; intelligent fiber; self-repair

1. Introduction

Brittle matrix composites such as ceramics, concrete, and brick are susceptible to cracking due to their low tensile strength, which can affect the overall mechanical performance and durability of the structures made of the composites [1–3]. Traditional repairing methods such as timed repair and after-the-fact repair can usually manage the visible cracks on the surface of some structural elements, but can hardly reach some cracks in complex structures. Self-repair or self-healing functionality of the composites, however, can provide timely repair to the structures and minimize the negative effect of cracks [3–5]—it is of great significance especially for the structures in complex environments such as space capsules, nuclear power plants, and marine tunnels.

Concrete is one of the most widely used construction materials. It is well known that concrete has some ability to self-heal [6]; its microdamage and microcracks caused by loads or environmental factors during the service time can be self-healed to some extent by further hydration of the unhydrated particles [7]. However, the self-healing efficiency of concrete seems to be low and the effect is limited by crack widths up to 200 μm [8–10]. To promote the self-repair or self-healing capacity of concrete, many techniques have been developed over the years, including: (1) Chemical self-healing techniques, such as mixing crystalline admixtures into concrete or brushing a layer of active admixture coating on the concrete surface [11–17], after water penetrates concrete through cracks, the active

functional group undergoes a condensation reaction and produces $CaCO_3$ crystals that fill the capillaries and microcracks in the concrete. When the concrete is again cracked, the active molecules are reactivated and continue to react until the cracks are healed. However, this method has minimal effect on repairing cracks over 400 μm in width [18–20]. (2) There are physical self-repair techniques, such as embedding shape memory alloy (SMA) into the crack-prone parts of concrete [21–30]; when cracks are generated, the electrical heating method is used to stimulate the shape recovery of SMA, forcing the cracks to close. However, the application scope of this technique is somewhat limited due to the relatively high investment in the external stimulation system and the expensive SMA. (3) Physical–chemical self-repair techniques, such as mixing the microencapsulated/hollow fibers (carriers) containing repair adhesive into concrete [31–44]—when cracks pass through the carrier, the repair agent flows out and penetrates into the cracks. The effect of this method is influenced by the number of carriers: fewer carriers are not enough to fill the cracks, while more carriers reduce the strength of the concrete. (4) Microbial self-healing techniques, such as adding specific harmless bacteria such as aerobic alkalophilic Bacillus into concrete [45–56]—as the concrete cracks, the infiltration of oxygen and water activates the dormant bacterial spores, and the process of microbial metabolism produces CO_2 that reacts with Ca^{2+} in the concrete to produce $CaCO_3$ crystals that seal and repair cracks up to 500 μm wide [57–59]; however, this method has some environmental and practical limitations because the bacteria have certain requirements concerning working environment and temperature. (5) Electrochemical self-repair techniques, such as the electrochemical deposition method, are generally achieved in an electric field where the positive and negative ions in the solution are deposited in the crack through an electrode reaction, producing insoluble crystals that fill the cracks [60–70]. However, this method requires the entire repair process to be electrified and the cost is relatively high.

As mentioned above, most of the current self-repair and self-healing techniques have repair limitations on crack width, or have an unfavorable effect on concrete strength, or need extra investment in an external stimulus. In contrast, the addition of fibers into concrete, though they cannot close or repair cracks, is helpful to control and reduce cracking and usually results in improved concrete strength and toughness, so it often combines with some self-repair or self-healing technique to achieve crack closure [3,71–76]. However, for the structures in corrosive environmental conditions, once the concrete is cracked, the harmful substances can enter through the cracks and rapidly corrode the reinforcement and cause overall degradation of structural integrity; in this case, the effect of the current self-repair or self-healing methods is even more limited. Based on these issues, we hope to develop a novel and relatively economical self-repair system that can enhance the durability of concrete structures under harsh environmental conditions.

This paper proposes a new concept of corrosion-induced intelligent fiber (CIF) and a new self-repairing system that uses the CIFs to close cracks in the brittle matrix composites within a corrosive environment without external help. The CIF can be prepared by coating the surface of the pre-tensioned core fiber with a corrosion-prone coating, then the CIFs can be embedded in the crack-prone parts of the brittle matrix composites. Once cracking occurs, the corrosive media in the environment penetrate through the cracks and trigger the shrinkage of the CIFs, which in turn releases the stored pre-stress to drive the cracks in the brittle matrix composites to close. Based on this concept, this paper also builds several mechanical models of the CIF and the self-repairing system to predict the magnitude of pre-stress stored in the core fiber, and the maximum pre-stress released to the brittle matrix composite, and the minimum length of the reliable anchor ends of CIF. This paper aims to provide the conceptual and theoretical development of the new CIF that can be efficient for closing cracks with a wide width range without external help, and without compromising strength, which has the potential to realize the intelligent functions of the brittle matrix composites in their feedback to external corrosion damage.

2. Corrosion-Induced Intelligent Fiber (CIF)

2.1. General Concept

The new CIF comprises an inner core fiber and an outer corrodible coating, wherein the core fiber is a corrosion-resistant material, and the corrodible coating can be easily corroded by corrosive media in the environment. The preparation steps of the CIF are shown in Figure 1. First, the core fiber is in an unstressed state (see Figure 1a), secondly, it is pre-tensioned in an elastic range, and the tensile stress is σ_0 (see Figure 1b), thirdly, the surface of the core fiber is uniformly coated with a corrodible coating by deposition, spraying, electroplating, or a similar process when the tensile stress σ_0 remains constant and the corrodible coating is in an unstressed state (see Figure 1c), and fourthly, the tensile force is removed after the coating is completed and cured. It is assumed that the core fiber is well bonded to the corrodible coating. In the process of removal, the corrodible coating is axially compressed under the elastic recovery force of the core fiber, and the compressive stress is σ_c^p (see Figure 1d). Finally, a tensile–compressive equilibrium is established between the corrodible coating and the core fiber, with the former in compression and the latter in tension.
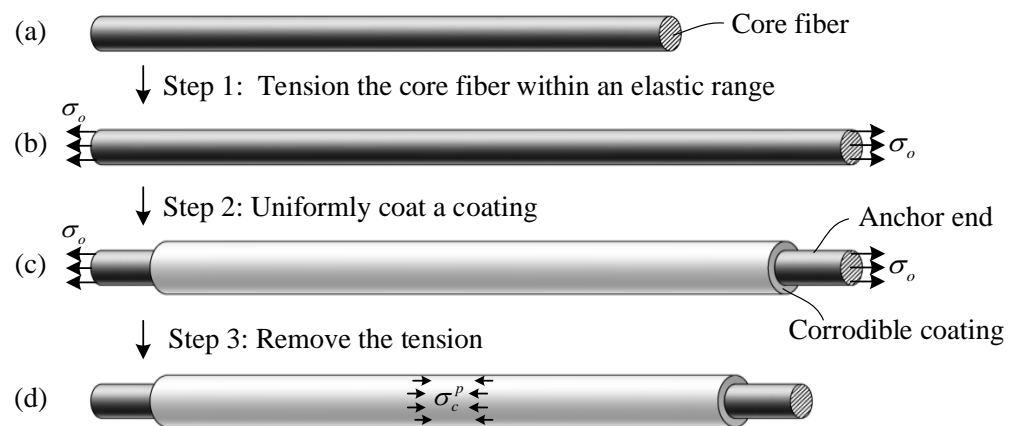

Figure 1. Schematic diagram of preparation process of the corrosion-induced intelligent fiber (CIF), (**a**) unstressed core fiber, (**b**) pre-tensioned core fiber, (**c**) pre-tensioned core fiber coated with an unstressed corrodible coating, (**d**) CIF in equilibrium with core fiber in tension and corrodible coating in compression.

2.2. Shape Recovery Mechanism of CIF

The shape recovery mechanism of the CIF is shown in Figure 2. When the environment is not corrosive, the CIF is not corroded, and the core fiber and the corrodible coating are in an original equilibrium state. In the corrosive environment, the corrodible coating in contact with the corrosive media forms a load-unbearable corrosion product, so the effective force section of the corrodible coating is decreasing, and the equilibrium state is broken; thus, the compressive stress and compressive deformation of the remaining corrodible coating increase constantly under the elastic recovery force of the core fiber, thereby the core fiber shrinks and gradually approaches its initial length, as shown in Figure 2b. Figure 2c shows that after the corrodible coating is corroded thoroughly, the pre-stress in the CIF is released and the core fiber recovers to the original length in an unstressed state.
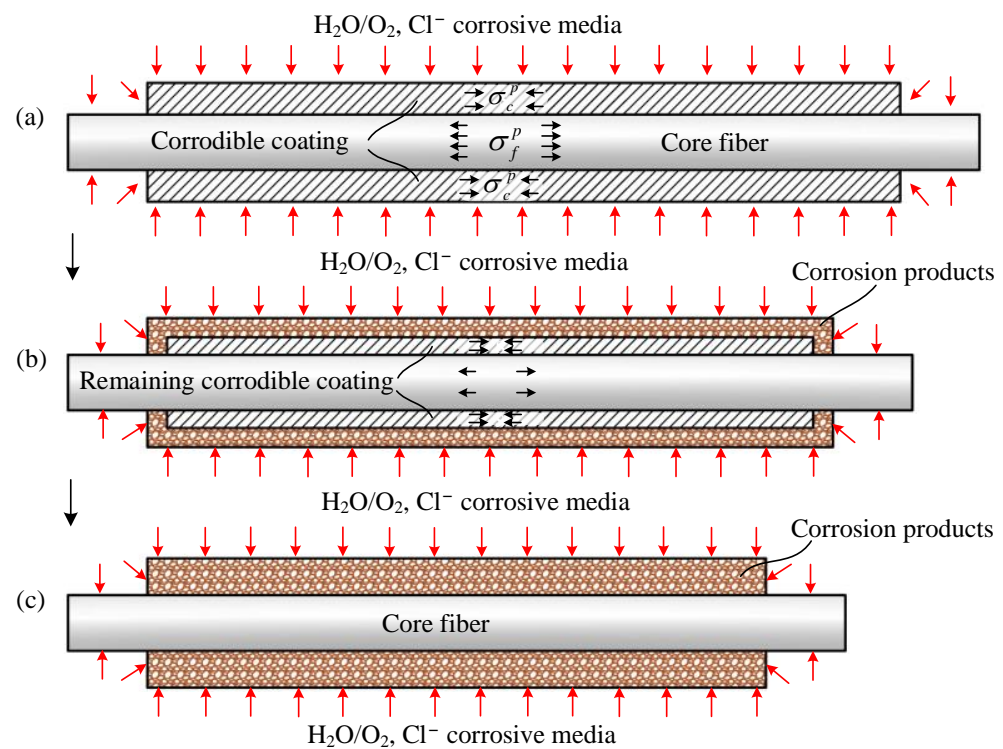
Figure 2. Axial cross-sectional view of the shape recovery mechanism of CIF, (**a**) CIF is in contact with corrosive media, (**b**) the effective force section of the corrodible coating decreases, the equilibrium is broken, and the core fiber shrinks, (**c**) core fiber recovers to the original length after the corrodible coating being corroded thoroughly.

3. Self-Repair Principle of CIF Composites

The CIF can be embedded in the crack-prone parts of the brittle matrix composite when applied in a corrosive environment. In order to transfer the pre-stress to the matrix composites more effectively, preferably the CIF reserve reliable anchor ends, such as uncoated bare ends, gradually thickening ends or end hooks. In the presence of the reliable anchor ends, whether the crack is distributed at the end portion of the CIF or the corrodible coating is completely corroded, the fiber is unlikely to be pulled out. The principle of self-repair of the CIF composites is shown in Figure 3. When the matrix composite cracks and the crack tips develop to the corrodible coating of the CIF, the corrosive media enter along the cracks and chemically or electrochemically react with the corrodible coating, and the CIF is triggered to shrink and transfers load through the bonding interface between the uncorroded CIF and the matrix composite to apply pressure to the matrix composite (see Figure 3b). It is clear that the higher corrosion degree of the corrodible coating, the larger crack closing force and a smaller crack width is generated. After the corrodible coating is corroded to a certain extent, the crack closing force is large enough, and the cracks are closed, as shown in Figure 3c; therefore, the inner passage for the corrosive media is cut off, and the corrosion is stopped, so the self-repair function is realized. At this time, the shrinkage of the CIF stops without increasing pressure to the brittle matrix composite.
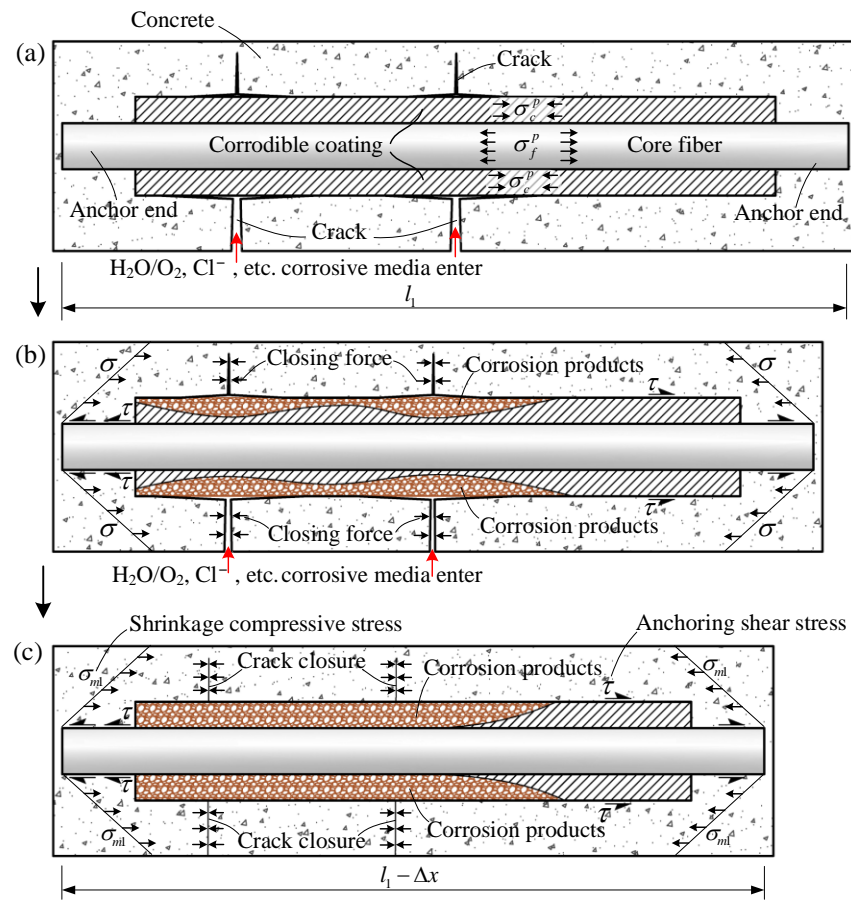
Figure 3. Axial cross-sectional view of the self-repair principle of the CIF composite, (**a**) corrosive media enter along the cracks and react with the corrodible coating, (**b**) CIF is triggered to shrink, the pre-stress stored in the core fiber is released to the matrix composite, (**c**) after the corrodible coating is corroded to a certain extent, the pressure applied to the matrix composite is large enough to close the cracks.

4. Derivation of the Mechanical Model

4.1. Mechanical Model of CIF

4.1.1. Basic Assumption

Since the CIF is a unidirectional composite with a large enough slenderness ratio, in order to simplify the calculation of internal force of the CIF, the following assumptions may be made:

1. The corrodible coating is evenly coated on the core fiber;
2. The core fiber and the corrodible coating are well bonded at the interface and the two have good chemical compatibility;
3. The influence of transverse strain of the core fiber and the corrodible coating is ignored and not incorporated into the Poisson's ratio in formula derivation;
4. The force of the core fiber and the corrodible coating is in a linear elastic state;
5. The structural unit is pulled positive and compressed negative.

4.1.2. Calculation of Internal Force

The symbols used in this section are listed in Table A1.

As shown in Figure 4, it is assumed that the original length of the core fiber that will be coated by the corrodible coating is l (see Figure 4a); in the pre-tensioning stage (see Figure 4b), the tensile stress is σ_0, and the elongation of the core fiber is Δx_1; in the coating stage (see Figure 4c), the length of the deposited coating is $l + \Delta x_1$. Owing to the recovery force of the core fiber after removing the pre-tension (see Figure 4d), the

compressive deformation of the coating is Δx_2, and the core fiber and the coating achieve force equilibrium and coordinated deformation. The tensile force of the core fiber is obtained according to Hooke's law as

$$F_f = \frac{E_f A_f}{l}(\Delta x_1 - \Delta x_2) \tag{1}$$

The pressure of the corrodible coating is

$$F_c = \frac{E_c A_c}{l + \Delta x_1}(-\Delta x_2) \tag{2}$$

The force equilibrium requires $F_f + F_c = 0$, that is

$$\frac{E_f A_f}{l}(\Delta x_1 - \Delta x_2) + \frac{E_c A_c}{l + \Delta x_1}(-\Delta x_2) = 0 \tag{3}$$

then

$$\Delta x_2 = \frac{E_f A_f \Delta x_1}{\frac{E_c A_c l}{l + \Delta x_1} + E_f A_f} \tag{4}$$

Since the compressive stress in the corrodible coating is

$$\sigma_c^p = E_c \varepsilon_c = E_c \frac{-\Delta x_2}{l + \Delta x_1} \tag{5}$$

Substituting Equation (4) into Equation (5) gives

$$\sigma_c^p = -\frac{E_c E_f A_f \Delta x_1}{E_c A_c l + E_f A_f (l + \Delta x_1)} \tag{6}$$

Supposing the cross-sectional area of the CIF is $A = A_c + A_f$, and simultaneously dividing the numerator and denominator on the right side of Equation (6) by Al, then

$$\sigma_c^p = -\frac{E_c E_f V_f \varepsilon_f}{E_c V_c + E_f V_f (1 + \varepsilon_f)} \tag{7}$$

where $\varepsilon_f = \Delta x_1 / l$; substituting $\varepsilon_f = \sigma_0 / E_f$ into Equation (7), then

$$\sigma_c^p = -\frac{E_c V_f \sigma_o}{E_c V_c + E_f V_f + V_f \sigma_o} \tag{8}$$

As σ_0 is much smaller than E_f, thus,

$$\sigma_c^p \approx -\frac{E_c V_f \sigma_o}{E_c V_c + E_f V_f} \tag{9}$$

At this point, the expression of pre-stress stored in the core fiber is

$$\sigma_f^p = -\frac{\sigma_c^p V_c}{V_f} = \frac{E_c V_c \sigma_o}{E_c V_c + E_f V_f} = \frac{E_c V_c \sigma_o}{E_1} \tag{10}$$

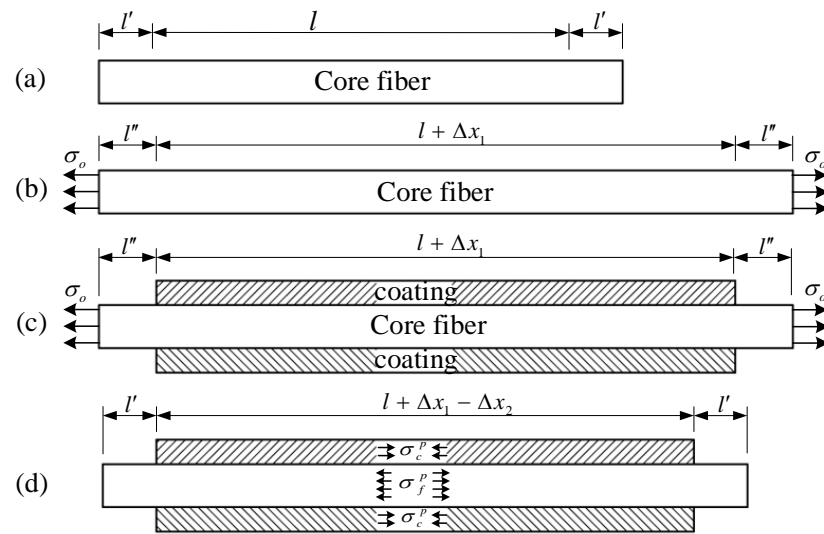where $E_1 = E_c V_c + E_f V_f$ is the composite elastic modulus, and $V_c + V_f = 1$.

Figure 4. The process diagram of CIF force equilibrium, (**a**) unstressed stage, (**b**) pre-tension stage, (**c**) coating stage, (**d**) external force withdrawal stage.

4.1.3. Force Storage Optimization

Based on Equation (10), the axial force F stored in the core fiber is

$$F = \sigma_f^p A_f = \frac{E_c V_c \sigma_o A_f}{E_c V_c + E_f V_f} = \frac{E_c V_c \sigma_o V_f A}{E_c V_c + E_f V_f} = \frac{(1 - V_f) V_f}{E_c (1 - V_f) + E_f V_f} E_c \sigma_o A \tag{11}$$

When F is maximum, the pre-stress released to the matrix composite is maximum. To solve the maximum value of the axial force of the core fiber, the F is first derived to obtain

$$F' = \frac{(1 - 2V_f) \left[E_c (1 - V_f) + E_f V_f \right] - (V_f - V_f^2)(E_f - E_c)}{\left[E_c (1 - V_f) + E_f V_f \right]^2} E_c \sigma_o A \tag{12}$$

that is

$$F' = \frac{(E_c - E_f) V_f^2 - 2E_c V_f + E_c}{\left[E_c (1 - V_f) + E_f V_f \right]^2} E_c \sigma_o A \tag{13}$$

When $F' = 0$, then

$$(E_c - E_f) V_f^2 - 2E_c V_f + E_c = 0 \tag{14}$$

When $E_c = E_f$, the F is maximum, and $V_f = 0.5$; when $E_c \neq E_f$, for the equation

$$V_f^2 - \frac{2E_c}{E_c - E_f} V_f + \frac{E_c}{E_c - E_f} = 0 \tag{15}$$

Assuming $a = \frac{E_C}{E_C - E_f}$, since $E_c > 0$ and $E_f > 0$, then $a < 0$ or $a > 1$, thus $\Delta = 4a^2 - 4a > 0$ and Equation (15) has two different real roots, which are

$$V_f = a \pm \sqrt{a^2 - a} = \frac{E_c \pm \sqrt{E_c E_f}}{E_c - E_f} = \frac{1 \pm \sqrt{E_f / E_c}}{1 - E_f / E_c} \tag{16}$$

Since the real root $V_f = \frac{1 + \sqrt{E_f / E_C}}{1 - E_f / E_C}$ does not satisfy the condition $0 < V_f < 1$, it should be discarded, while the other real root

$$V_f = \frac{E_c - \sqrt{E_c E_f}}{E_c - E_f} \tag{17}$$

satisfies the condition and gives the maximum axial force storage F_{max}.

4.2. Mechanical Model of CIF Composites

The permanent anchor ends of CIF are the portion of the core fiber not coated with the corrodible coating, or the portion where the surface of the core fiber with corrodible coating is coated with the corrosion-resistant coating; the length of any permanent anchor end is defined as l'. When the CIF reserved with permanent anchor ends is added into the matrix composite, the pre-stress released to the matrix composite can be predicted when the shrinkage of CIF stops.

4.2.1. Basic Assumption

In order to simplify the calculation of interaction between the CIF and the brittle matrix composite, the following assumptions are made:

1. The CIF is unidirectionally and uniformly arranged in the matrix composite;
2. The influence of the Poisson's ratio on the magnitude of the axial stress is disregarded;
3. The permanent anchor ends are tightly bonded with the matrix composite without slippage;
4. The force influence of the corrosion product of the corrodible coating is disregarded.

4.2.2. Calculation of Internal Force

The symbols used in this section are listed in Table A2.

After the cross-section of the corrodible coating is completely lost, the pre-stress released to the brittle matrix composite by the shrinkage of the core fiber is maximum. As the corrosion product does not participate in the force, the core fiber and the brittle matrix composite establish a final tensile–compressive equilibrium. According to Equation (9), it can be known that the pre-stress released to the matrix composite by the shrinkage of the core fiber is

$$\sigma_m^p = -\frac{E_m \frac{V_{f1}}{1-V_{c1}} \sigma_f^p}{E_2} = -\frac{E_m V_{f1} \sigma_f^p}{E_f V_{f1} + E_m V_m} \tag{18}$$

At this point, the tensile stress in the core fiber is

$$\sigma_{f1}^p = \frac{E_m V_m \sigma_f^p}{E_f V_{f1} + E_m V_m} \tag{19}$$

where E_2 is the composite elastic modulus of the brittle matrix composite with the core fiber, and $E_2 = E_f V_{f1}/(1 - V_{c1}) + E_m V_m/(1 - V_{c1})$, $V_{f1} + V_{c1} = V_s$, and $V_s + V_m = 1$.

4.2.3. Anchor Length of CIF

In order that the permanent anchor ends are reliable without slipping, a sufficient length is required. It is assumed that the bonding anchoring force of the permanent anchor end is $T_a = \tau \pi d l'$, and the drawing force of the CIF is $T_t = \sigma_{f1}^p \pi d^2/4$. According to the force equilibrium $T_a = T_t$, the following is obtained

$$l' = \frac{d \sigma_{f1}^p}{4\tau} \tag{20}$$

where τ is the bonding stress between the CIF and the matrix composite at the interface, and when the composition and properties of the matrix composite and the CIF are known, τ can be determined; l' is the anchor length (the length of one end) of the CIF in the brittle matrix composite, and d is the diameter of the cross-section of the anchor end.

Formula (19) is substituted into Equation (20) to obtain

$$l' = \frac{d\sigma_{f1}^p}{4\tau} = \frac{dE_m V_m \sigma_f^p}{4\tau \left(E_f V_{f1} + E_m V_m \right)} \tag{21}$$

If the permanent anchor end is reliable for effectively transferring the pre-stress to the matrix composite without slipping, then

$$l' \geq \frac{dE_m V_m \sigma_f^p}{4\tau \left(E_f V_{f1} + E_m V_m \right)} \tag{22}$$

Thus, for the given material parameters of the CIF and the matrix composite, and the given volume fraction, the minimum length of the reliable anchor end of the CIF can be confirmed by calculation.

5. Discussion

Based on the concept of CIF, the self-repair method of the CIF composites has obvious advantages. First, the CIF composites working in a corrosive environment are capable of self-repairing without external help and independent of temperature, so compared to the self-repair techniques using SMA or an electric field, the use of CIF in concrete can reduce the costs. Second, the larger the pre-stress stored in the core fiber, or the higher corrosion degree the corrodible coating encounters, the larger the crack closure force that can be released to the concrete, meaning a wider crack can be repaired; thus, compared to the self-healing or self-repair techniques using crystalline admixtures, microcapsules, or bacteria, the use of CIF in concrete can close cracks with a wider width range without compromising the strength of the concrete. Third, before the corrodible coating is corroded thoroughly, when the concrete is again cracked, the corrodible coating can continue to be corroded until the cracks are closed or the cross-section of the corrodible coating is completely lost. Fourth, the use of CIF in concrete can act as effective reinforcement both before and after corrosion.

Based on the derived mechanical models, we can predict the self-repair capacity of the CIF composite. For example, we set the material of the corrodible coating of the CIF to be iron, the core fiber of the CIF to be a copper-plated steel fiber or a nylon fiber with a diameter of 0.2 mm (regardless of copper plating amount), and set the matrix composite to be concrete in a chloride environment. The material parameters of CIF and concrete are listed in Table 1. According to Section 4.1.3, if $E_c = E_f$, the maximum axial force stored in the core fiber (F_{max}) is obtained when the volume fraction of the core fiber in the CIF was 50%; if $E_c \neq E_f$, the F_{max} is obtained when the volume fraction of the core fiber is determined according to Equation (17). Setting the amount of CIFs in concrete (V_s) to be 4V%, and assuming that the CIF is unidirectionally and uniformly arranged in the concrete, then the pre-stress stored in the core fiber (σ_f^p) and the maximum pre-stress released to the concrete (σ_m^p) are calculated according to Equations (10) and (18), respectively. The recoverable strain of the core fiber (ε_f^p) can be calculated according to $\varepsilon_f^p = \sigma_f^p / E_f$. The results are shown in Table 1.

From the above sample calculation, it can be shown that, after the iron coating of the CIF is lost due to chloride corrosion, the recovery strain of the core fiber is 0.5% for the steel fiber and 12.7% for the nylon fiber. That is, if the length of the CIF is 20 mm, the recovery strain can be 2.5 mm for the CIF with the nylon core fiber, which means, if the CIF concrete member is free of external force, the theoretical crack closure width can be up to 2.5 mm. It can also be seen from Table 1 that the maximum pre-stress released to the concrete is 18.6 MPa for the CIF with the steel core fiber and 24.5 MPa for the CIF with the nylon core fiber. Figure 5 shows that when the amount of CIFs (V_s) and the initial tensile stress of the core fiber (σ_0) continuously increase, the maximum compressive stress applied to concrete also continuously increases. Thus, for the given composition and properties of the concrete

and the CIF, the crack closing force provided by the CIF to concrete can be increased by increasing V_s and σ_0.

Table 1. Basic material parameters and calculation results of CIF and concrete.

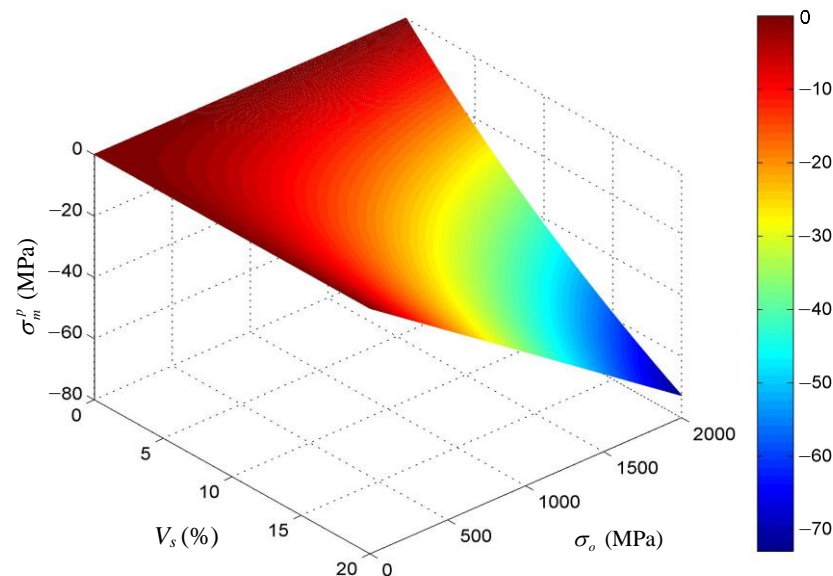| No. | Composition | Material | Parameters | | | σ_f^p (MPa) | ε_f^p | σ_m^p (MPa) |
			E (GPa)	V_{f1}	σ_o (MPa)			
1	Corrodible coating	Iron	200	50% × 4%	-	-	-	-
	Core fiber	Steel	200	50% × 4%	2000	1000	0.5%	−18.6
	Matrix	Concrete	35	96%	-	-	-	-
2	Corrodible coating	Iron	200	14% × 4%	-	-	-	-
	Core fiber	Nylon	5.4 [77]	86% × 4%	800	687	12.7%	−24.5
	Matrix	Concrete	35	96%	-	-	-	-

Figure 5. The influence of the amount of CIFs (V_s) and the initial tensile stress (σ_0) on the maximum pre-stress released to concrete (σ_m^p).

The application of CIF will benefit crack closure, increase rigidity, and improve the corrosion resistance of concrete. This paper only provides the conceptual and theoretical study of the CIF and CIF composites; many important issues remain for future study. First, the performance of the self-repairing system and the optimization of the composition and properties of the CIF need to be explained via finite element analysis. Second, the optimized CIF needs to be prepared in the laboratory and explored with a set of experiments that can show the self-repairing behavior of the CIF composite within a corrosive environment.

6. Conclusions

This paper presents a new concept of CIF that comprises an inner corrosion-resistant core fiber and an outer corrodible coating that can be easily corroded by corrosive media in the environment. During preparation process, the inner core fiber is put into tension and the outer corrodible coating into compression, such that the CIF is in equilibrium. When the CIF is in contact with corrosive media, the outer corrodible coating is corroded, and the core fiber shrinks and displays shape recovery, which in turn releases the pre-tension stress in the core fiber. By far, shape memory fibers comprising core fibers coated with a corrosion-resistant compound/material are well known, but a shape memory fiber by coating a corrodible coating on a core fiber has not yet been reported.

This paper also proposes a new self-repairing system that uses the CIFs to close cracks in brittle matrix composites within a corrosive environment. Once cracking occurs, the CIFs embedded in the matrix composite can be triggered to shrink by the corrosive media from the environment, which in turn releases the pre-stress stored in the core fiber and thereby applies a compressive force to the matrix composite that acts to close the cracks. By far, self-repair concrete comprising reinforcing fibers is well known, but not with a corrodible coating in equilibrium with the core fiber. Compared to the current self-repair or self-healing techniques for concrete, the use of CIF in concrete can cost less than using SMA or the electrochemical deposition method because it is independent of temperature and does not need external help. Furthermore, it can be more efficient for closing wider cracks than that provided by the crystalline admixtures, microcapsules, or bacteria methods, all of which have unfavorable effect on concrete strength. Additionally, the use of CIF in brittle matrix composite can act as effective reinforcement both before and after corrosion.

Based on the concepts, this paper also builds several mechanical models to predict the magnitude of pre-stress stored in the core fiber, the maximum pre-stress released to the brittle matrix composite, and the minimum length of the reliable anchor ends of CIF. These aim to attain an optimum combination of the CIF and matrix composite to provide enough crack closing force. Based on a sample calculation, the recovery strain was 0.5% for CIF with a steel core fiber and 12.7% for CIF with a nylon core fiber. The maximum crack closing force provided by the CIF to concrete can be increased by increasing the amount of CIFs in concrete and the initial tensile stress of the core fiber.

The presence of CIF can be helpful toward improving the crack resistance of concrete, especially the low-modulus polymer fiber concrete. It can help to reduce the probability of premature concrete cracking and improve the durability of the concrete structures in corrosive environments, including marine and underground environments. For the future work, many important issues related to the concepts need to be explored. First, the optimization of the composition and properties of the CIF needs to be found via finite element analysis before performing the time-consuming laboratory tests; second, the optimized CIF needs to be prepared in the laboratory; and third, a set of experiments should be conducted to explore the self-repairing behavior of the CIF composite within actual corrosive environments.

Author Contributions: Conceptualization, Z.W.; Methodology, Z.W.; Validation, Y.S.; Writing—original draft, Y.S. and D.W.; Writing—review and editing, Z.J. and J.S. All authors have read and agreed to the published version of the manuscript.

Institutional Review Board Statement: Not applicable.

Data Availability Statement: No new data were created or analyzed in this study. Data sharing is not applicable to this article.

Conflicts of Interest: The authors declare no conflict of interest.

Appendix A.

Table A1. Symbols in formula deduction for the corrosion-induced intelligent fiber (CIF).

Symbol	Description
E_f	elastic modulus of the core fiber
E_c	elastic modulus of the corrodible coating
A_f	cross-sectional area of the core fiber
A_c	cross-sectional area of the corrodible coating
ε_f	initial tensile strain of the core fiber
ε_c	strain of the corrodible coating after equilibrium
V_f	volume fraction of the core fiber in the CIF
V_c	volume fraction of the corrodible coating in the CIF
E_1	elastic modulus of the CIF
σ_0	pre-tensile stress in the core fiber
σ_f^p	pre-stress stored in the core fiber after equilibrium
σ_c^p	compressive stress in the corrodible coating after equilibrium

Table A2. Symbols in formula deduction for CIF composites.

Symbol	Description
E_m	elastic modulus of the brittle matrix composite
E_2	composite elastic modulus of the matrix composite with the core fiber
V_{f1}	volume fraction of the core fiber in the CIF composite
V_{c1}	volume fraction of the corrodible coating in the CIF composite
V_s	volume fraction of the CIFs in the CIF composite
V_m	volume fraction of the matrix composite in the CIF composite
σ_m^p	pre-stress released to the brittle matrix composite after equilibrium
σ_{f1}^p	tensile stress in the core fiber after equilibrium

References

1. Jamari, J.; Ammarullah, M.I.; Santoso, G.; Sugiharto, S.; Supriyono, T.; van der Heide, E. In Silico Contact Pressure of Metal-on-Metal Total Hip Implant with Different Materials Subjected to Gait Loading. *Metals* **2022**, *12*, 1241. [CrossRef]
2. De Nardi, C.; Cecchi, A.; Ferrara, L. The Influence of Self-Healing Capacity of Lime Mortars on the Behaviour of Brick-Mortar Masonry Subassemblies. *Key Eng. Mater.* **2017**, *747*, 465–471. [CrossRef]
3. Maddalena, R.; Bonanno, L.; Balzano, B.; Tuinea-Bobe, C.; Sweeney, J.; Mihai, I. A crack closure system for cementitious composite materials using knotted shape memory polymer (k-SMP) fibres. *Cem. Concr. Compos.* **2020**, *114*, 103757. [CrossRef]
4. Greil, P. Self-Healing Engineering Ceramics with Oxidation-Induced Crack Repair. *Adv. Eng. Mater.* **2020**, *22*, 1901121. [CrossRef]
5. Albuhairi, D.; Di Sarno, L. Low-Carbon Self-Healing Concrete: State-of-the-Art, Challenges and Opportunities. *Buildings* **2022**, *12*, 1196. [CrossRef]
6. Hearn, N. *Saturated Permeability of Concrete as Influenced by Cracking and Self-Sealing*; University of Cambridge: Cambridge, UK, 1993.
7. Hearn, N.; Morley, C.T. Self-sealing property of concrete—Experimental evidence. *Mater. Struct./Mater. Constr.* **1997**, *30*, 404–411. [CrossRef]
8. Roig-Flores, M.; Serna, P. Concrete Early-Age Crack Closing by Autogenous Healing. *Sustainability* **2020**, *12*, 4476. [CrossRef]
9. Qureshi, T.; Al-Tabbaa, A. *Self-Healing Concrete and Cementitious Materials*; Chapter 12; IntechOpen: London, UK, 2020; pp. 191–214. [CrossRef]
10. De Belie, N.; Gruyaert, E.; Al-Tabbaa, A.; Antonaci, P.; Baera, C.; Bajare, D.; Darquennes, A.; Davies, R.; Ferrara, L.; Jefferson, T.; et al. A Review of Self-Healing Concrete for Damage Management of Structures. *Adv. Mater. Interfaces* **2018**, *5*, 1800074. [CrossRef]
11. Edvardsen, C. Water Permeability and Autogenous Healing of Cracks in Concrete. *Mater. J.* **1999**, *96*, 448–454. [CrossRef]
12. Ziegler, F.; Masuero, A.B.; Pagnussat, D.T.; Molin, D.C.C.D. Evaluation of Internal and Superficial Self-Healing of Cracks in Concrete with Crystalline Admixtures. *Materials* **2020**, *13*, 4947. [CrossRef]
13. Li, G.; Huang, X.; Lin, J.; Jiang, X.; Zhang, X. Activated chemicals of cementitious capillary crystalline waterproofing materials and their self-healing behaviour. *Constr. Build. Mater.* **2019**, *200*, 36–45. [CrossRef]
14. Ravitheja, A.; Reddy, T.; Sashidhar, C. Self-healing concrete with crystalline admixture—A review. *J. Wuhan Univ. Technol.-Mater. Sci. Ed.* **2019**, *34*, 1143–1154. [CrossRef]
15. Zhang, C.; Lu, R.; Li, Y.; Guan, X. Effect of crystalline admixtures on mechanical, self-healing and transport properties of engineered cementitious composite. *Cem. Concr. Compos.* **2021**, *124*, 104256. [CrossRef]

16. Xue, C.; Li, W.; Qu, F.; Sun, Z.; Shah, S.P. Self-healing efficiency and crack closure of smart cementitious composite with crystalline admixture and structural polyurethane. *Constr. Build. Mater.* **2020**, *260*, 119955. [CrossRef]

17. Žáková, H.; Pazderka, J.; Reiterman, P. Textile reinforced concrete in combination with improved self-healing ability caused by crystalline admixture. *Materials* **2020**, *13*, 5787. [CrossRef]

18. Sisomphon, K.; Copuroglu, O.; Koenders, E. Self-healing of surface cracks in mortars with expansive additive and crystalline additive. *Cem. Concr. Compos.* **2012**, *34*, 566–574. [CrossRef]

19. De Souza Oliveira, A.; Gomes, O.d.F.M.; Ferrara, L.; Fairbairn, E.d.M.R.; Toledo Filho, R.D. An overview of a twofold effect of crystalline admixtures in cement-based materials: From permeability-reducers to self-healing stimulators. *J. Build. Eng.* **2021**, *41*, 102400. [CrossRef]

20. Roig-Flores, M.; Pirritano, F.; Serna, P.; Ferrara, L. Effect of crystalline admixtures on the self-healing capability of early-age concrete studied by means of permeability and crack closing tests. *Constr. Build. Mater.* **2016**, *114*, 447–457. [CrossRef]

21. Song, G.; Ma, N.; Li, H.N. Applications of shape memory alloys in civil structures. *Eng. Struct.* **2006**, *28*, 1266–1274. [CrossRef]

22. Siddiquee, K.N.; Billah, A.H.M.M.; Issa, A. Seismic collapse safety and response modification factor of concrete frame buildings reinforced with superelastic shape memory alloy (SMA) rebar. *J. Build. Eng.* **2021**, *42*, 102468. [CrossRef]

23. Abdulridha, A.; Palermo, D.; Foo, S.; Vecchio, F.J. Behavior and modeling of superelastic shape memory alloy reinforced concrete beams. *Eng. Struct.* **2013**, *49*, 893–904. [CrossRef]

24. Kuang, Y.; Ou, J. Self-repairing performance of concrete beams strengthened using superelastic SMA wires in combination with adhesives released from hollow fibers. *Smart Mater. Struct.* **2008**, *17*, 025020. [CrossRef]

25. Mohd Jani, J.; Leary, M.; Subic, A.; Gibson, M.A. A review of shape memory alloy research, applications and opportunities. *Mater. Des.* **2014**, *56*, 1078–1113. [CrossRef]

26. Furuya, Y.; Sasaki, A.; Taya, M. Enhanced mechanical properties of TiNi shape memory fiber/Al matrix composite. *Mater. Trans. JIM* **1993**, *34*, 224–227. [CrossRef]

27. Chen, W.; Feng, K.; Wang, Y.; Lin, Y.; Qian, H. Evaluation of self-healing performance of a smart composite material (SMA-ECC). *Constr. Build. Mater.* **2021**, *290*, 123216. [CrossRef]

28. Cohades, A.; Hostettler, N.; Pauchard, M.; Plummer, C.J.G.; Michaud, V. Stitched shape memory alloy wires enhance damage recovery in self-healing fibre-reinforced polymer composites. *Compos. Sci. Technol.* **2018**, *161*, 22–31. [CrossRef]

29. Geetha, S.; Selvakumar, M. A composite for the Future-Concrete Composite Reinforced with Shape Memory Alloy Fibres. *Mater. Today Proc.* **2019**, *18*, 5550–5555. [CrossRef]

30. Jia, Y.-q.; Lu, Z.-D.; Li, L.-Z.; Wu, Z.-L. A Review of Applications and Research of Shape Memory Alloys in Civil Engineering. *IOP Conf. Ser. Mater. Sci. Eng.* **2018**, *392*, 022009. [CrossRef]

31. Dry, C. Procedures developed for self-repair of polymer matrix composite materials. *Compos. Struct.* **1996**, *35*, 263–269. [CrossRef]

32. White, S.R.; Sottos, N.R.; Geubelle, P.H.; Moore, J.S.; Kessler, M.R.; Sriram, S.; Brown, E.N.; Viswanathan, S. Autonomic healing of polymer composites. *Nature* **2001**, *409*, 794–797. [CrossRef]

33. Zotiadis, C.; Patrikalos, I.; Loukaidou, V.; Korres, D.M.; Karantonis, A.; Vouyiouka, S. Self-healing coatings based on poly(urea-formaldehyde) microcapsules: In situ polymerization, capsule properties and application. *Prog. Org. Coat.* **2021**, *161*, 106475. [CrossRef]

34. Rule, J.D.; Sottos, N.R.; White, S.R. Effect of microcapsule size on the performance of self-healing polymers. *Polymer* **2007**, *48*, 3520–3529. [CrossRef]

35. Wang, J.Y.; Soens, H.; Verstraete, W.; De Belie, N. Self-healing concrete by use of microencapsulated bacterial spores. *Cem. Concr. Res.* **2014**, *56*, 139–152. [CrossRef]

36. Dubey, R.; Shami, T.C.; Bhasker Rao, K.U. Microencapsulation technology and applications. *Def. Sci. J.* **2009**, *59*, 82–95. [CrossRef]

37. Bonilla, L.; Hassan, M.M.; Noorvand, H.; Rupnow, T.; Okeil, A. Dual self-healing mechanisms with microcapsules and shape memory alloys in reinforced concrete. *J. Mater. Civ. Eng.* **2018**, *30*, 04017227. [CrossRef]

38. Aghamirzadeh, G.R.; Khalili, S.M.R.; Eslami-Farsani, R.; Saeedi, A. Experimental investigation on the smart self-healing composites based on the short hollow glass fibers and shape memory alloy strips. *Polym. Compos.* **2019**, *40*, 1883–1889. [CrossRef]

39. Li, W.; Jiang, Z.; Yu, Q. Multiple damaging and self-healing properties of cement paste incorporating microcapsules. *Constr. Build. Mater.* **2020**, *255*, 119302. [CrossRef]

40. Wang, Y.; Lin, Z.; Tang, C.; Hao, W. Influencing factors on the healing performance of microcapsule self-healing concrete. *Materials* **2021**, *14*, 4139. [CrossRef]

41. Jiang, S.; Lin, Z.; Tang, C.; Hao, W. Preparation and mechanical properties of microcapsule-based self-healing cementitious composites. *Materials* **2021**, *14*, 4866. [CrossRef]

42. Castaneda, H.; Hassan, M.M.; Radovic, M.; Milla, J.; Karayan, A. *Self-Healing Microcapsules as Concrete Aggregates for Corrosion Inhibition in Reinforced Concrete*; Transportation Consortium of South-Central States: Washington, DC, USA, 2018.

43. Pulikkalparambil, H.; Sanjay, M.; Siengchin, S.; Khan, A.; Jawaid, M.; Pruncu, C.I. Self-repairing hollow-fiber polymer composites. In *Woodhead Publishing Series in Composites Science and Engineering, Self-Healing Composite Materials*; Woodhead Publishing: Sawston, UK, 2020; pp. 313–326. [CrossRef]

44. Feng, J.; Dong, H.; Wang, R.; Su, Y. A novel capsule by poly (ethylene glycol) granulation for self-healing concrete. *Cem. Concr. Res.* **2020**, *133*, 106053. [CrossRef]

45. Luo, M.; Qian, C.-X.; Li, R.-Y. Factors affecting crack repairing capacity of bacteria-based self-healing concrete. *Constr. Build. Mater.* **2015**, *87*, 1–7. [CrossRef]

46. Luo, M.; Qian, C. Influences of bacteria-based self-healing agents on cementitious materials hydration kinetics and compressive strength. *Constr. Build. Mater.* **2016**, *121*, 659–663. [CrossRef]

47. Van Tittelboom, K.; De Belie, N.; De Muynck, W.; Verstraete, W. Use of bacteria to repair cracks in concrete. *Cem. Concr. Res.* **2010**, *40*, 157–166. [CrossRef]

48. Wiktor, V.; Jonkers, H.M. Quantification of crack-healing in novel bacteria-based self-healing concrete. *Cem. Concr. Compos.* **2011**, *33*, 763–770. [CrossRef]

49. Intarasoontron, J.; Pungrasmi, W.; Nuaklong, P.; Jongvivatsakul, P.; Likitlersuang, S. Comparing performances of MICP bacterial vegetative cell and microencapsulated bacterial spore methods on concrete crack healing. *Constr. Build. Mater.* **2021**, *302*, 124227. [CrossRef]

50. Allahyari, H.; Heidarpour, A.; Shayan, A. Experimental and analytical studies of bacterial self-healing concrete subjected to alkali-silica-reaction. *Constr. Build. Mater.* **2021**, *310*, 125149. [CrossRef]

51. Zhang, X.; Qian, C. Engineering application of microbial self-healing concrete in lock channel wall. *Mar. Georesources Geotechnol.* **2022**, *40*, 96–103. [CrossRef]

52. Sri Durga, C.S.; Ruben, N.; Sri Rama Chand, M.; Indira, M.; Venkatesh, C. Comprehensive microbiological studies on screening bacteria for self-healing concrete. *Materialia* **2021**, *15*, 101051. [CrossRef]

53. Chen, X.; Yuan, J.; Alazhari, M. Effect of microbiological growth components for bacteria-based self-healing on the properties of cement mortar. *Materials* **2019**, *12*, 1303. [CrossRef]

54. Van Wylick, A.; Monclaro, A.V.; Elsacker, E.; Vandelook, S.; Rahier, H.; De Laet, L.; Cannella, D.; Peeters, E. A review on the potential of filamentous fungi for microbial self-healing of concrete. *Fungal Biol. Biotechnol.* **2021**, *8*, 16. [CrossRef]

55. Feng, C.; Zong, X.; Cui, B.; Guo, H.; Zhang, W.; Zhu, J. Application of Carrier Materials in Self-Healing Cement-Based Materials Based on Microbial-Induced Mineralization. *Crystals* **2022**, *12*, 797. [CrossRef]

56. Onyelowe, K.C.; Ebid, A.M.; Riofrio, A.; Baykara, H.; Soleymani, A.; Mahdi, H.A.; Jahangir, H.; Ibe, K. Multi-Objective Prediction of the Mechanical Properties and Environmental Impact Appraisals of Self-Healing Concrete for Sustainable Structures. *Sustainability* **2022**, *14*, 9573. [CrossRef]

57. Eran, Y.C.; Hernandez-Sanabria, E.; Boon, N.; De Belie, N. Enhanced crack closure performance of microbial mortar through nitrate reduction. *Cem. Concr. Compos.* **2016**, *70*, 159–170. [CrossRef]

58. Palin, D.; Wiktor, V.; Jonkers, H.M. A bacteria-based self-healing cementitious composite for application in low-temperature marine environments. *Biomimetics* **2017**, *2*, 13. [CrossRef]

59. Erşan, Y.Ç.; Gruyaert, E.; Louis, G.; Lors, C.; De Belie, N.; Boon, N. Self-protected nitrate reducing culture for intrinsic repair of concrete cracks. *Front. Microbiol.* **2015**, *6*, 1228. [CrossRef]

60. Chu, H.-Q.; Jiang, L.-H.; Yu, L. Effect of electrodeposition on BET surface area and microstructure of cement mortar. *J. Build. Mater.* **2006**, *9*, 627–632. (In Chinese)

61. Goux, A.; Pauporte, T.; Chivot, J.; Lincot, D. Temperature effects on ZnO electrodeposition. *Electrochim. Acta* **2005**, *50*, 2239–2248. [CrossRef]

62. Otsuki, N.; Ryu, J.S. Use of electrodeposition for repair of concrete with shrinkage cracks. *J. Mater. Civ. Eng.* **2001**, *13*, 136–142. [CrossRef]

63. Kim, J.-K.; Yee, J.-J.; Kee, S.-H. Electrochemical deposition treatment (Edt) as a comprehensive rehabilitation method for corrosion-induced deterioration in concrete with various severity levels. *Sensors* **2021**, *21*, 6287. [CrossRef]

64. Ryu, J.-S.; Otsuki, N. Crack closure of reinforced concrete by electrodeposition technique. *Cem. Concr. Res.* **2002**, *32*, 159–164. [CrossRef]

65. Yan, Z.; Chen, Q.; Zhu, H.; Woody Ju, J.; Zhou, S.; Jiang, Z. A multi-phase micromechanical model for unsaturated concrete repaired using the electrochemical deposition method. *Int. J. Solids Struct.* **2013**, *50*, 3875–3885. [CrossRef]

66. Liu, L.; Dong, B. Investigation of concrete crack repair by electrochemical deposition. *Int. J. Electrochem. Sci.* **2021**, *16*, 2. [CrossRef]

67. Wang, Y.; Wang, C.; Zhou, S.; Liu, K. Influence of Anode Material on the Effect of Electrophoretic Deposition for the Repair of Rust-Cracked Reinforced Concrete. *Constr. Build. Mater.* **2022**, *335*, 127466. [CrossRef]

68. Zhu, H.; Chen, Q.; Ju, J.W.; Yan, Z.; Jiang, Z. Electrochemical deposition induced continuum damage-healing framework for the cementitious composite. *Int. J. Damage Mech.* **2021**, *30*, 945–963. [CrossRef]

69. Yang, Q.; Wang, J.; Yuan, L.; Zhou, Z. Effect of graphene and carbon fiber on repairing crack of concrete by electrodeposition. *Ceram.-Silik.* **2019**, *63*, 403–412. [CrossRef]

70. Wang, C.; Wang, Y.; Liu, K.; Zhou, S. Effect of colloid solution concentration of epoxy resin on properties of rust-cracked reinforced concrete repaired by electrophoretic deposition. *Constr. Build. Mater.* **2022**, *318*, 126184. [CrossRef]

71. Cuenca, E.; Ferrara, L. Self-healing capacity of fiber reinforced cementitious composites. State of the art and perspectives. *KSCE J. Civ. Eng.* **2017**, *21*, 2777–2789. [CrossRef]

72. Liu, H.; Zhang, Q.; Gu, C.; Su, H.; Li, V. Influence of microcrack self-healing behavior on the permeability of Engineered Cementitious Composites. *Cem. Concr. Compos.* **2017**, *82*, 14–22. [CrossRef]

73. Wang, D.; Ju, Y.; Shen, H.; Xu, L. Mechanical properties of high performance concrete reinforced with basalt fiber and polypropy-lene fiber. *Constr. Build. Mater.* **2019**, *197*, 464–473. [CrossRef]

74. Balzano, B.; Sweeney, J.; Thompson, G.; Tuinea-Bobe, C.-L.; Jefferson, A. Enhanced concrete crack closure with hybrid shape memory polymer tendons. *Eng. Struct.* **2021**, *226*, 111330. [CrossRef]
75. Garg, M.; Azarsa, P.; Gupta, R. Self-healing potential and post-cracking tensile behavior of polypropylene fiber-reinforced cementitious composites. *J. Compos. Sci.* **2021**, *5*, 122. [CrossRef]
76. Wei, M.; Zhong, K.; Cai, S.; Feng, T.; Zhang, N. Preparation and application of the novel resin microcapsules in self-repairing cement composites with polypropylene fibers. *J. Adhes. Sci. Technol.* **2022**, 1–20. [CrossRef]
77. Ahmad, J.; Zaid, O.; Aslam, F.; Shahzaib, M.; Ullah, R.; Alabduljabbar, H.; Khedher, K.M. A study on the mechanical characteristics of glass and nylon fiber reinforced peach shell lightweight concrete. *Materials* **2021**, *14*, 4488. [CrossRef] [PubMed]